

## ASSESSMENT OF THE ACCURACY OF TWO DIFFERENT SCANNING APPROACHES FOR THE AURICULAR DEFECT

Mohamed Y. Abdelfattah\*<sup>ID</sup>, Marwa Amer\*\*<sup>ID</sup> and Maha Maged\*\*<sup>ID</sup>

### ABSTRACT

**Aim:** The objective of the current study was to compare the accuracy of digital impression technique for auricular defects using two different techniques. The study aims to determine which digital impression can provide comparable or superior accuracy, precision, and reliability.

**Materials and Methods:** Seven patients with auricular defects were selected from the outpatient Prosthodontic clinic seeking auricular prostheses. For each patient three digital impressions were taken for the auricular defect: the first was taken by IOS without resin markers, The second was taken by IOS with placement of similar resin marker, the third was taken by IOS with placement of dissimilar resin marker. The accuracy of both techniques (intraoral scanning with similar or dissimilar markers) can then be assessed by comparing those scans with intraoral scanning without resin markers using Meshcompare software.

**Results:** highly significant differences were recorded in between both techniques concerning total 3d dimensional deviation.

**Conclusion:** IOS with dissimilar resin skin markers can produce a much more accurate and cost-effective digital impressions for auricular defects.

**Clinical Significance:** The digital intraoral scanning of the auricular defect side with skin markers offers a fast accurate technique for the rehabilitation of ear defects, permitting a base for additional investigations in the field of maxillofacial prosthodontics.

**KEYWORDS:** Digital Impression, IOS, Simillar and dissimilar Skin Markers

\* Assistant Professor of Prosthodontics, Department of Prosthodontics, Faculty of Dentistry, Tanta University,

\*\* Lecturer of Prosthodontics, Department of Prosthodontics, Faculty of Dentistry, Tanta University,

## INTRODUCTION

Maxillofacial defects either arise from congenital conditions, trauma, or tumor resection have a significant impact on a person's physical, functional, and psychosocial well-being. Prosthetic rehabilitation permits restoration of esthetics, and functions that improve patient satisfaction and social integration.<sup>1</sup> Facial prosthesis is conventionally constructed using numerous complex long steps that could disturb the patient and depend on maxillofacial team skills. Impression taking using alginate or silicone is associated with high risk of inaccuracy due to movement of the skin and the load of the impression material which distort the impression.<sup>2,3</sup>

Digital technologies are now increasingly used to simplify the production of facial prostheses with the advantages of producing fast, high quality and enhanced functional and aesthetic outcomes. This can be achieved by 3-D scanning of the soft tissue and generating mirror-imaged anatomical replicas, then by direct 3D printing of the definitive prosthesis in medical grade silicon or a 3-d printing of the negative mold for the fabrication of prostheses.<sup>4,5</sup> Progression in scanning techniques and digital systems either at the CT or MRI levels or surface scanners such as 3d photogrammetry, intraoral scanners, facial scanners, or laser scanners with the aid of specialized medical software.<sup>6,8</sup> can deliver precise topographical information of the patients without tissues contact. Thus eliminate the problems of the conventional impressions<sup>9,10</sup> Data acquisition regarding the defect area and its contralateral side is the primary and greatest significant phase as it regulates the result of the prosthesis particularly ear prosthesis which is very challenging due to the unusually complex auricle structure, that contains numerous undercuts and creases that are tough to be reproduced.<sup>11</sup>

IOS are used for portraying photosensitive images in dental field and their precision is

clinically acceptable. Believing their precision and convenience, IOS can be applied to obtain comprehensive surface texture for maxillofacial prosthesis. Scanning markers can be attached to the skin areas that are smooth and devoid of features to facilitate the stitching process and increase the scanning accuracy.<sup>5,12,13</sup> Numerous studies described the usage of IOS with a marker or an indicator to produce a rapid and precise digital auricular impression either for construction of ear prostheses or for locating the position of auricular implant with the assistance of scan bodies and to make auricular templates for creating a three dimensions cartilaginous framework for ear reconstruction.<sup>5,8,14,15,16</sup> Intraoral scanners also granted a precise diagnostic measure for assessing the effectiveness of any treatment of ear defects.<sup>17,18</sup>

Only few Studies evaluating the accuracy of various digital data acquisition techniques. This research compares intraoral scanning with/without external similar and dissimilar scanning markers. The null hypothesis is that there are no significant differences between digital impression techniques using IOS with similar or dissimilar markers for the auricular defect.

## MATERIAL & METHODS

In this study, seven patients with auricular defects were selected from the outpatient Prosthodontics Department's clinic, Faculty of Dentistry, Tanta University seeking auricular prostheses. The study was accomplished after obtaining the authorization of the Ethical Committee at the Faculty of Dentistry, Tanta University, Egypt (#R-RP-5-24-3105). All included patients signed an informed written consent. For each patient three digital intraoral scanning were taken for the auricular defect (the first was taken by IOS without resin markers, The second was taken by IOS with placement of similar resin marker, the third was taken by IOS with placement of dissimilar resin marker.

### Sample size:

The minimum required sample size was decided to be seven patients/group. The sample size was calculated using the G Power software version 3.1.9.2.24.<sup>19</sup>

#### *A- Digital intraoral scanning of the auricular defect without resin markers:*

Using Alliedstar intraoral scanner (Alliedstar AS 100) the auricular defect (Figure 1) was scanned starting from the center of the present rudimentary ear (to be the initial, final, and as reference points for auricular scan) then moving upwards, posteriorly, downwards, and anteriorly and after each time we returned to the reference point again till complete the scan of the defect area.

#### *B- Digital intraoral scanning of the auricular defect with resin markers: 19*

Resin markers with different shapes (Figure 2) were designed using free Blender software (blender-4.2.0-windows-x64.msi). The markers were created using SAVOY 3d printing resin (SAVOY Digital systems C&B Resin) with Anycubic 3d printer (Anycubic Photon S - High-precision SLA 3D Resin). The markers are considered to be reference points throughout the scan process, creating enhanced, improved photographing records. The markers can simply be eliminated from the digital framework without adopting the precision of the scanning process. These markers were arranged around the rudimentary ear (above, posteriorly, and below it). After the intraoral scanning without resin marker was finished. Similar resin markers were adhered using medical adhesive (Pros-Aide adhesive medical grade) mainly posterior and below the center of the defect (Figure 3) and the scanning was done with the same technique after that different resin markers were used in the same way. The scanned files were exported as a Standard Tessellation Language (STL) file format.



Fig. (1): Auricular defect side.



Fig. (2): 3d printed resin markers with different shapes.



Fig. (3): similar skin markers were adhered in place.

**C- Digital comparison of different data acquisition techniques:**

Using Alliedstar Meshcompare package, the IOS without markers of the auricular defects were determined as references for all forthcoming assessments. Then, finest-appropriate arrangement procedures were employed to index the digital scan with similar resin markers on the reference data and the same was done for the digital scan with dissimilar resin markers (Figure 4 and 6). Then a

3D surface comparison was evaluated. The total 3D deviation was recorded at the center, above, below, posteriorly, and anteriorly. The deviation was represented as color map from the least deviation (green color 0.000-0.200) to outward deviation (yellow to red) or inward deviation (light blue to dark blue) (Figure 5 and 7). Ten points were recorded at each area and the mean was taken. Then the total deviation from the reference data (without resin markers) was recorded for both similar and dissimilar resin markers.

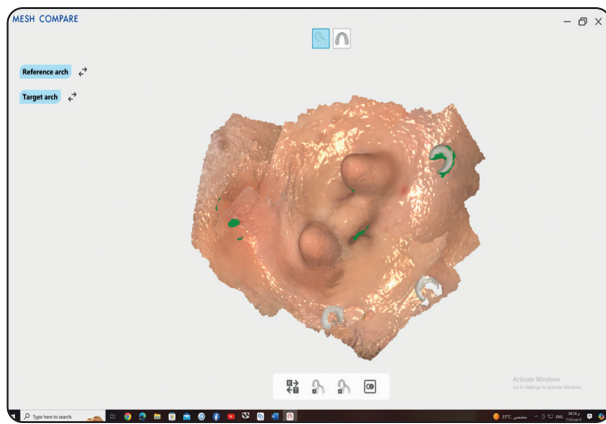


Fig. (4) Superimposition of the digital intraoral auricular defect scanning without markers and scanning with similar markers.

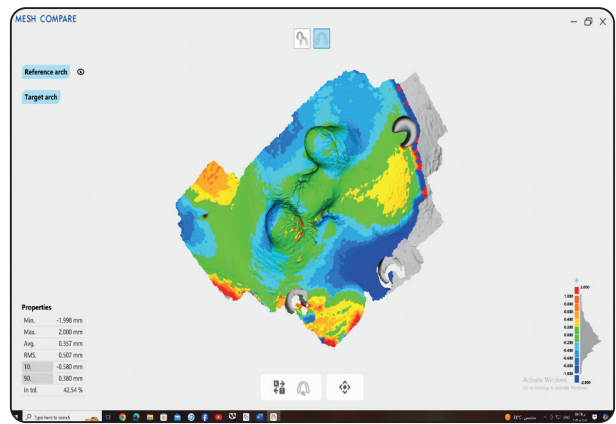


Fig. (5) Color map showing comparison between digital intraoral auricular defect scanning without markers and scanning with similar markers.

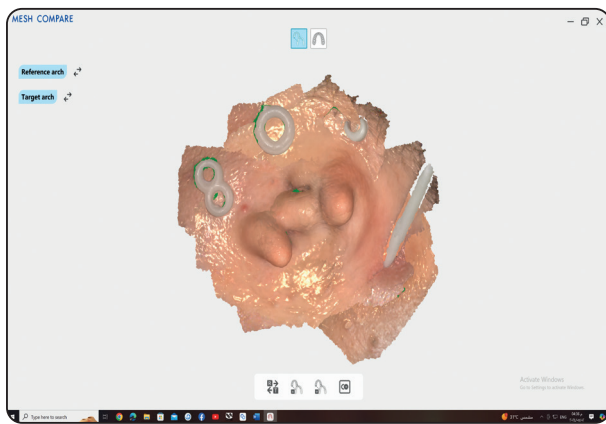


Fig. (6) Superimposition of the digital intraoral auricular defect scanning without markers and scanning with dissimilar markers.

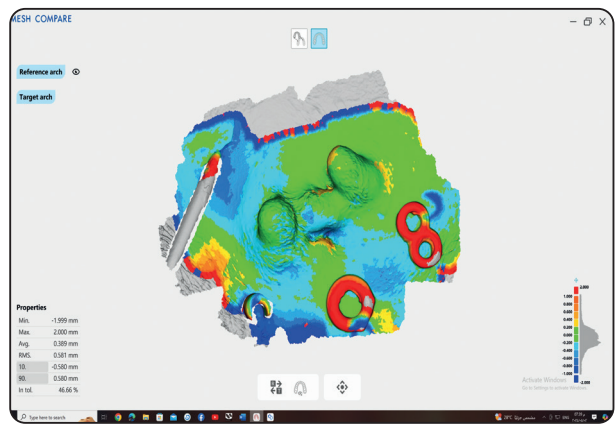


Fig. (7) Color map showing comparison between digital intraoral auricular defect scanning without markers and scanning with dissimilar markers.



### Statistical analyses

Statistical Package for Social Sciences (IBM SPSS Statistics version 26) was used to analyze the results. Numerical variables are expressed by mean, standard deviation and range, where nominal data are expressed using frequency and percentage. P value <0.05(\*) was indicated as significant difference & P-value <0.001(\*\*) was thought highly significant difference. The tests used in this analysis for parametric variables: The Shapiro-Wilk test is used to check the normality of the data and the independent t-test is used to compare the studied group at each duration.

### RESULTS

The outcomes of the current investigation declined the null hypothesis and authorized the presence of highly significant differences between IOS with similar resin marker and with dissimilar resin marker. The colour map of the superimposed changes between the intraoral ear defect scan in addition that using similar markers is displayed in (Figures 4 and 6) and that with dissimilar resin markers is shown in (Figure 5 and 7). The blue zones designate surface warp and compression, while red zones denote space between the two compared STL files. The perfect scanning believed

to exhibit additional zones of green colour that specify similar assessed STL files, providing zero measurement values. The normality of collected data were examined using Shapiro-Wilk test (Table 1). The scans were compared at different areas (center, anterior, posterior, above, and below) by selection of ten points at each area and calculate the mean. The results of this study, which is expressed using mean, standard deviation, and range, show the comparison between intraoral scan without marker vs with similar marker group and intraoral scan without marker vs dissimilar resin marker group at each area individually using independent t-test, which displayed highly significant differences between them with P-value 0.000\*\* at center point, anterior, posterior, above, and below, with more deviation for dissimilar marker group at the center, anterior, and above areas and with more deviation for the similar marker group at the posterior and below areas (Table 2).

The total 3D deviation between the two groups, which is expressed using mean, standard deviation, and range, showed that the least deviation results for the dissimilar marker group with highly significant differences with P-value 0.0000\*\* when compared with the similar marker group (Table 3).

TABLE (1) Shows the Shapiro-Wilk test is used to examine the normality of the data, since the data is normal.

Point	Intraoral scan without marker vs with similar marker	Intraoral scan without marker vs with dissimilar marker
	Shapiro-Wilk (p-value)	Shapiro-Wilk (p-value)
Centre	0.870 (0.186)	0.856(0.139)
Anterior	0.916(0.435)	0.897(0.392)
Posterior	0.817(0.083)	0.940(0.640)
Above	0.818(0.063)	0.961(0.814)
Below	0.874(0.199)	0.902(0.346)

*There is a significant at P-value< 0.05 (\*), and highly significant at P-value< 0.001 (\*\*).*

TABLE (2) Shows the 3d deviation results at the center, anterior, posterior, above, and below areas in similar and dissimilar marker groups.

Point	Intra vs similar resin marker		Intra vs dissimilar resin marker		Independent t-test T (p-value)
	Mean ±S.D	Range	Mean ±S.D	Range	
Centre	0.127±0.008	119—139	0.201±0.002	0.199—0.205	24.486(0.000**)
Anterior	0.176±0.003	0.169—0.180	0.194±0.003	0.191—0.201	10.192(0.000**)
Posterior	0.351±0.007	0.335—0.355	0.213±0.001	0.210—0.215	49.928(0.000**)
Above	0.213±0.005	0.206—0.224	0.258±0.011	0.257—0.260	21.425(0.000**)
Below	0.191±0.001	0.189—0.193	0.128±0.003	0.125—0.134	50.744(0.000**)

*There is a significant at P-value< 0.05 (\*), and highly significant at P-value< 0.001 (\*\*).*

TABLE (3) Shows the total 3d deviation results between the similar and the dissimilar marker groups.

Point	Intra vs similar resin marker		Intra vs dissimilar resin marker		Independent t-test t (p-value)
	Mean ±S.D	Range	Mean ±S.D	Range	
Total	0.211±0.001	0.210—0.213	0.199±0.001	0.197—0.199	24.052(0.000**)

*There is a significant at P-value< 0.05 (\*), and highly significant at P-value< 0.001 (\*\*).*

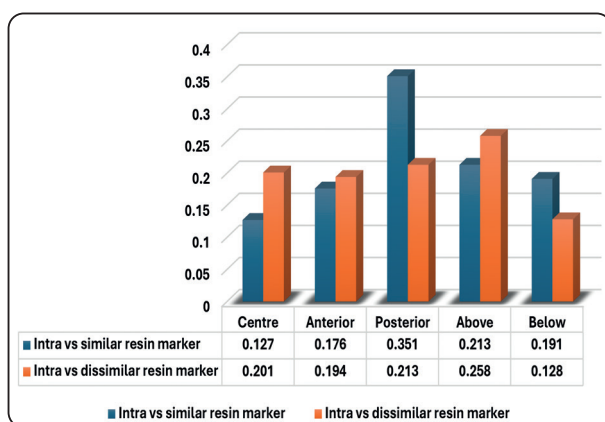


Diagram (1): Shows the 3d deviation results at the center, anterior, posterior, above, and below areas in similar and dissimilar marker groups.

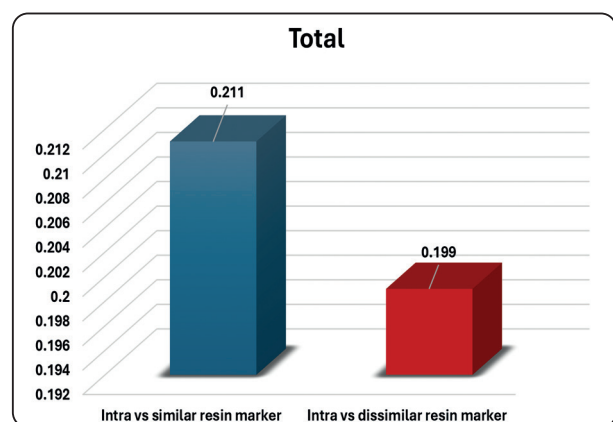


Diagram (2): Shows the total 3d deviation results between the similar and the dissimilar marker groups.

## DISCUSSION

The overall three-dimension deviation in intraoral auricular defect scanning with similar resin markers was highly statistically significant from that with dissimilar markers. Current research suggests an improved technique to obtain digital soft tissue data of ear defects, which permit construction of precise ear prostheses with great adaptation to the defect side due to the accuracy of the collected data. Auricular defect scanning using intraoral scanner provides more precise data than the traditional impressions of the normal and defect auricles. Deficiency of sufficient generation of minor parts and surface texture, poor dimensional stability, and patient discomfort, are the main drawbacks of conventional impressions as compared to digital options. This was in accordance with Burzynski et al<sup>20</sup> who presumed that the IOS were superior when compared with the typical hydrocolloid impressions. This is also in agreement with Dohiem et al<sup>19</sup> who found that utilizing IOS allows data acquisition and provide better precision than conventional impression techniques. Together with the presence of skin markers enhance the speed of scanning in addition to creating more accurate outcomes, reducing sewing difficulties that impact the precision of scans endured without markers. This fact is also supported by Mai HN and Lee DH<sup>21</sup> Who found that the precision of simulated maxillofacial incorporation was mostly varied with the usage of peri-oral scanning and skin markers and the minimum eccentricity were noted when the perioral image with artificial markers were utilized. Following keloid tissue surgical amputation Nejat AH et al<sup>22</sup> fabricated rapid (2-3 minutes) and accurate 3D printed ear splints using IOS and markers to prevent further regrowth of the keloid. Similarly, Ballo AM et al<sup>5</sup> have defined a precise technique for creating digital ear impressions quickly using intraoral scanners and markers, providing a detailed method for accurate results. The use of dissimilar skin markers was supposed to be more accurate

than the similar markers as confirmed by the current research outcomes. Total 3-D deviation of the scans using dissimilar skin markers is less than that with similar markers, with highly significant difference, when compared with the intraoral scan of the auricular defect without markers (Diagram 2). This may be attributed to the less stitching complication and the more accurate collected data with using dissimilar skin markers than with similar skin markers during intraoral scanning of the auricular defect as demonstrated by the results of this study (Table 3). The outcomes of current investigation also found that 3-D scanning deviation using dissimilar skin markers was less than that with similar markers when compared to the intraoral scan without skin markers at the posterior and inferior areas with highly significant difference (Diagram 1). This may be attributed to the distribution of skin markers in this study was selected to be more at the posterior and the below areas due to the less skin details at these sites with more difficult scanning and more stitching problems than the other areas. In another study, artificial markers were strategically placed on several flat areas with weakly distinguished landmarks, ensuring that the distances between the markers were approximately similar. This method facilitated more precise stitching of the captured images, thereby enhancing the accuracy of the digital impressions. This approach is particularly useful in areas where natural landmarks are less distinct, improving the overall quality and reliability of the digital modeling process.<sup>19</sup> These markers, once placed and used to enhance the precision of the digital impressions, could easily be removed from the recorded virtual image. This ensures that the final digital model is both accurate and clean, without the artificial markers interfering with the visual quality of the model.<sup>5, 11, 23, 24</sup> This was confirmed also by the results of the other areas (center, anterior, and superior) where the 3d deviation of the dissimilar skin markers is more than that of similar markers when compared with the intraoral scanning without

markers, this may be due to the deficient numbers of skin markers at those areas (Diagram 1). The challenges encountered while using intraoral scanners (IOS) for extraoral scanning, such as the difficulty in stitching obtained images, often stem from the lack of obvious landmarks on soft tissues compared to the distinct landmarks found on tooth morphology during intraoral scanning. This issue was addressed by applying resin markers and employing a specific scanning pattern. The remaining ear structure, with its complex anatomy, was used as the starting and finishing reference, effectively resolving the problem of stitching the acquired data. This approach ensured accurate and seamless digital impressions of the ear.<sup>5</sup> Cone beam computed tomography (CBCT) and extraoral optical scanners are alternative modalities used for acquiring data on the auricle and auricular defects. However, these techniques come with certain limitations. For instance, they often fail to capture the detailed texture of the skin, which is crucial for accurate modeling. Extraoral optical scanners, in particular, require prolonged scanning periods, making them susceptible to distortions caused by any uncontrolled head movements during the process. Additionally, these scanners typically struggle to capture data from the rear of the site, leading to incomplete or inaccurate representations.<sup>5, 8, 25</sup> Data recorded using CBCT scan often suffer from low resolution, primarily due to the segmentation process of Digital Imaging and Communication in Medicine (DICOM) files when converting them into Standard Tessellation Language (STL) files. This reduction in resolution can affect the accuracy and detail of the final 3D model. Additionally, CBCT scanning carries potential radiation hazards, which is a concern when considering its use, especially in non-essential cases or for patients requiring multiple scans.<sup>5, 8, 11, 25-27</sup> In the study, the intraoral scanner without markers served as the control group, as it has been recognized by many authors as an effective and accurate scanning method, often

surpassing the conventional impression techniques. The use of intraoral scanners is widely accepted for their precision and efficiency in capturing detailed digital impressions, making them a reliable standard for comparison in this research.

In this study, Meshcompare software was utilized to compare the collected data, specifically using the Allied Star Meshcompare software for 3D inspection and metrology. Mohammed et al.<sup>28</sup> previously compared the accuracy of different conventional auricular impression techniques by measuring the distance between fixed points on the ear surface, a method that does not account for the deformity and compressibility of soft tissue. In contrast, the present study's use of Meshcompare software offers a more reliable approach, as it employs the best-fit alignment algorithm, which has been reported by many authors to result in low alignment errors and accurate measurements of comparison points. This method ensures a more precise comparison between different scans, enhancing the overall validity of the study's findings.<sup>29,30</sup> Blender software, which was used for resin marker design in this study, is a versatile free-form modeling software widely recognized for its applications in accurately designing dental prosthetics. Its flexibility and precision make it an ideal tool for creating detailed and customized models, contributing to the accuracy and effectiveness of digital workflows in various medical and dental applications.<sup>31-33</sup> The skin resin markers were 3-D printed in this study as it saves time, with low cost, less waste material, and biocompatible as supported by other studies.<sup>34, 35</sup>

## CONCLUSIONS

IOS represents a significant accurate and cost-effective technique for recording digital impressions of auricular defects. Applying dissimilar resin skin markers minimize errors through permitting for much more meticulous data acquisition ensuring high-quality, accurate, more reliable and detailed digital scans.



## Funding

This research did not receive any specific grant from funding agencies in the public, commercial, or not-for-profit sectors.

## REFERENCES

1. Beumer J III, Marunick MT, Garrett N. Rehabilitation of maxillary defects. In: Beumer J III, Marunick MT, Esposito SJ (eds). *Maxillofacial Rehabilitation: Prosthodontic and Surgical Management of Cancer-Related, Acquired, and Congenital Defects of the Head and Neck*, ed 3. Chicago: Quintessence, 2011:155–212.
2. Karakoca S, Aydin C, Yilmaz H, Korkmaz T. An impression technique for implant-retained orbital prostheses. *J Prosthet Dent* 2008 Jul 1;100(1):52–55.
3. Kubon TM, Anderson JD. An implant-retained auricular impression technique to minimize soft tissue distortion. *J Prosthet Dent* 2003 Jan 1;89(1):97–101.
4. Farook TH, Jamayet NB, Abdullah JY, Asif JA, Rajion ZA, Alam MK. Designing 3D prosthetic templates for maxillofacial defect rehabilitation: A comparative analysis of different virtual workflows. *Comput Biol Med* 2020 Mar 1;118:103646.
5. Ballo AM, Nguyen CT, Lee VSK. Digital workflow of auricular rehabilitation: A technical report using an intraoral scanner. *J Prosthodont* 2019;28(5):596–600.
6. Yunpeng Bi, Minghao Zhou, Hongbo Wei. Digital workflow for auricular prosthesis fabrication with a negative mold. *J Prosthet Dent* 2024;131:1254–1258.
7. Elbashti ME, Sumita YI, Kelimu S, Aswehlee AM, Awuti S, Hattori M, et al. Application of digital technologies in maxillofacial prosthetics literature: A 10-year observation of five selected prosthodontics journals. *Int J Prosthodont* 2019;32:45–50.
8. Bannink T, Bouman S, Wolterink R, van Veen R, van Alphen M. Implementation of 3D technologies in the workflow of auricular prosthetics: A method using optical scanning and stereolithography 3D printing. *J Prosthet Dent* 2021;125:708–713.
9. Germec-Cakan D, Canter HI, Nur B, Arun T. Comparison of facial soft tissue measurements on three-dimensional images and models obtained with different methods. *J Craniofac Surg*. 2010;21:1393–1399.
10. Runte C, Dirksen D, Deleré H, Thomas C, Runte B, Meyer U, et al. Optical data acquisition for computer-assisted design of facial prostheses. *Int J Prosthodont* 2002;15:129–132.
11. Liu H, Bai S, Yu X, Zhao Y. Combined use of a facial scanner and an intraoral scanner to acquire a digital scan for the fabrication of an orbital prosthesis. *J Prosthet Dent* 2019;121(3):531–534.
12. Wang S, Leng X, Zheng Y, Zhang D, Wu G. Prosthesis-guided implant restoration of an auricular defect using computed tomography and 3-dimensional photographic imaging technologies: A clinical report. *J Prosthodont* 2015;113:152–156.
13. Unkovskiy A, Wahl E, Huettig F, Keutel C, Spintzyk S. Multimaterial. 3D printing of a definitive silicone auricular prosthesis: An improved technique. *J Prosthet Dent* 2021;125:946–950.
14. Dashti H, Rajati Haghi H, Nakhaei M, Kiamanesh E. A combined digital technique to fabricate an implant-retained auricular prosthesis for rehabilitation of hemifacial microsomia. *J Prosthet Dent* 2021:1–4.
15. Lang Z, Xiong T, Wang M, Chu Y. A simple and accurate method for the production of a personalized two-dimensional auricular template. *Aesthetic Plast Surg* 2020;44(3):1106–1107.
16. Liao J, Chen Y, Chen J, He B, Qian L, Xu J, et al. Auricle shaping using 3D printing and autologous diced cartilage. *Laryngoscope* 2019;129(11):2467–2474.
17. Britto J, Panchal P, Prasad A, Kumari R, Kumari S. Photogrammetric morphometric analysis of auricle. *Int J Med Sci Public Heal* 2018 Jun 1;7(6):1.
18. Wang D, Jiang H, Pan B, Yang Q, He L, Sun H, et al. Standardized measurement of auricle: A method of high-precision and reliability based on 3D scanning and Mimics software. *Exp Ther Med* 2019:4575–4582.
19. Dohiem MM, Emam NS, Abdallah MF, Abdelaziz MS. Accuracy of digital auricular impression using intraoral scanner versus conventional impression technique for ear rehabilitation: a controlled clinical trial. *Journal of Plastic, Reconstructive & Aesthetic Surgery*. 2022 Nov 1;75(11):4254–4263.
20. Burzynski JA, Firestone AR, Beck FM, Fields Jr HW, Deguchi T. Comparison of digital intraoral scanners and alginate impressions: Time and patient satisfaction. *Am J Orthod Dentofac Orthop* 2018;153:534–541.

21. Mai HN, Lee DH. The Effect of Perioral Scan and Artificial Skin Markers on the Accuracy of Virtual Dentofacial Integration: Stereophotogrammetry Versus Smartphone Three-Dimensional Face-Scanning. *Int J Environ Res Public Health* 2020 Dec 30;18(1):229.
22. Nejat AH, Hamdan S, Abrego I, Lindsey JT, Vitter R. Fully digital workflow for fabrication of a 3D printed ear stent for auricular keloids: A technique article. *J Prosthodont* 2022;31(3):266–270.
23. Unkovskiy A, Brom J, Huettig FKC. Auricular prostheses produced using conventional and digital workflows: A clinical report on esthetic outcomes. *Int J Prosthodont* 2018;31:63–66.
24. Ciocca L, Mingucci R, Gassino GSR. CAD/CAM ear model and virtual construction of the mold. *J Prosthet Dent* 2007;98:339–343.
25. Liacouras P, Ganes J, Roman N, Petrich AGG. Designing and manufacturing an auricular prosthesis using computed tomography, 3-dimensional photographic imaging, and additive manufacturing: A clinical report. *J Prosthet Dent* 2011;105:78–82.
26. Bai SZ, Feng ZH, Gao R, Dong Y, Bi YP, Wu GF, et al. Development and application of a rapid rehabilitation system for reconstruction of maxillofacial soft-tissue defects related to war and traumatic injuries. *Mil Med Res* 2014;1:11.
27. Hassan B, Gimenez Gonzalez B, Tahmaseb A, Greven MWD. A digital approach integrating facial scanning in a CAD-CAM workflow for complete-mouth implant-supported rehabilitation of patients with edentulism: A pilot clinical study. *J Prosthet Dent* 2017;117:486–492.
28. Mohamed K, Mani UM, Seenivasan MK, Vaidhyanathan AK, Veeravalli PT. Comparison of two impression techniques for auricular prosthesis: Pilot study. *J Rehabil Res Dev* 2013;50(8):1079–1087.
29. Son K, Lee WS, Lee KB. Effect of different software programs on the accuracy of dental scanner using three-dimensional analysis. *Int J Environ Res Public Health* 2021;18(16).
30. O'Toole S, Osnes C, Bartlett D, Keeling A. Investigation into the accuracy and measurement methods of sequential 3D dental scan alignment. *Dent Mater* 2019;35(3):495–500.
31. Farook TH, Barman A, Abdullah JY, Jamayet NB. Optimization of Prosthodontic Computer-Aided Designed Models: A Virtual Evaluation of Mesh Quality Reduction Using Open Source Software. *J Prosthodont* 2021 Jun;30(5):420-429.
32. Abad-Coronel C, Pazán DP, Hidalgo L, Larriva Loyola J. Comparative analysis between 3D-printed models designed with generic and dental-specific software. *Dent J* 2023 Sep 14;11(9):216.
33. Uyar A, Pişkin B, Pişkin M, Akın H, Arısan V, Koçyiğit Ö. Evaluation of The Processing Discrepancies Between Dental and Nondental CAD Software Using The Smoothing Design Tool. *Acta stomatologica cappadocia* 2022;2(1):18-36.
34. Mai HN, Lee DH. Effects of Artificial Extraoral Markers on Accuracy of Three-Dimensional Dentofacial Image Integration: Smartphone Face Scan versus Stereophotogrammetry. *J Pers Med* 2022;12:490.
35. Guttridge C, Shannon A, O'Sullivan A, O'Sullivan KJ, O'Sullivan LW. Biocompatible 3D printing resins for medical applications: A review of marketed intended use, biocompatibility certification, and post-processing guidance. *Ann 3D Print Med* 2022;5(100044):2666-9641.